Protein Science (1998), 7:2602–2612. Cambridge University Press. Printed in the USA.

Localization of basic residues required for receptor binding to the single α-helix of the receptor binding domain of human α_2-macroglobulin

WEN HUANG, KLAVS DOLMER, XIUBEI LIAO, AND PETER G.W. GETTINS

Department of Biochemistry and Molecular Biology, College of Medicine, University of Illinois at Chicago, Chicago, Illinois 60612-4316

(RECEIVED April 9, 1998; ACCEPTED August 12, 1998)

Abstract

To better understand the structural basis for the binding of proteinase-transformed human α_2-macroglobulin (α_2M) to its receptor, we have used three-dimensional multinuclear NMR spectroscopy to determine the secondary structure of the receptor binding domain (RBD) of human α_2M. Assignment of the backbone NMR resonances of RBD was made using $^{13}C/^{15}N$ and ^{15}N-enriched RBD expressed in *Escherichia coli*. The secondary structure of RBD was determined using ^{1}H and ^{13}C chemical shift indices and inter- and intrachain nuclear Overhauser enhancements. The secondary structure consists of eight strands in β-conformation and one α-helix, which together comprise 44% of the protein. The β-strands form three regions of antiparallel β-sheet. The two lysines previously identified as being critical for receptor binding are located in (Lys1374), and immediately adjacent to (Lys1370) the α-helix, which also contains an (Arg1378). Secondary structure predictions of other α-macroglobulins show the conservation of this α-helix and suggest an important role for this helix and for basic residues within it for receptor binding.

Keywords: α_2-macroglobulin; LRP; NMR; receptor binding domain; receptor recognition; secondary structure

Human α_2-macroglobulin (α_2M) is an abundant broad-specificity plasma proteinase inhibitor that inhibits proteinases by physically sequestering them as a consequence of a massive proteinase-initiated conformational change (Barrett & Starkey, 1973; Barrett et al., 1979; Sottrup-Jensen, 1989). This conformational change also results in exposure of the receptor binding region (Tapon-Bretaudiere et al., 1985) and consequent binding of the α_2M-proteinase complexes to cell-surface receptor and rapid internalization by receptor-mediated endocytosis (Maxfield et al., 1981; Hanover et al., 1983; Yamashiro et al., 1989). The receptor binding region of α_2M has been localized to a discrete 138 residue C-terminal domain, which can be quantitatively isolated from plasma α_2M by limited proteolytic cleavage (Sottrup-Jensen et al., 1986; Van Leuven et al., 1986). This domain is termed the receptor binding domain (RBD). The receptor to which α_2M-proteinase complexes bind is a 550 kDa membrane-spanning protein that has been shown to be the largest member of the low density lipoprotein receptor family (Herz et al., 1988; Kristensen et al., 1990; Strickland et al., 1990). Its relationship to the low density lipoprotein receptor has earned it the sesquipedalian name of low density lipoprotein receptor-related protein, which is more conveniently abbreviated to LRP. LRP is a multifunctional receptor (Strickland et al., 1995) that binds not only α_2M-proteinase complexes but many other proteins including certain serpin-proteinase complexes (Orth et al., 1992; Nykjær et al., 1992; Poller et al., 1995; Kounnas et al., 1996; Strickland & Kounnas, 1997), lipoprotein lipase (Nykjær et al., 1993), apoE-enriched remnant lipoproteins (Kowal et al., 1989), lactoferrin (Willnow et al., 1992), *Pseudomonas aeruginosa* exotoxin A (Kounnas et al., 1992), and a protein that copurifies with LRP and is accordingly called receptor associated protein (RAP) (Williams et al., 1992).

LRP is biosynthesized as a single chain that is subsequently processed into a heterodimer composed of a C-terminal 601 residue light-chain (β) and an N-terminal 3923 residue heavy chain (α) (Herz et al., 1990). The β-chain comprises a small cytoplasmic domain, a single transmembrane helix, and an extracellular domain that has seven copies of an EGF-like repeat. The α-chain contains an additional 15 single or tandem EGF-like repeats interspersed among 31 complement-like repeats grouped in clusters of 2–11 repeats and seven clusters of five YWTD-containing repeats. It is thought likely that the ability of LRP to bind such a diverse array of ligands is related to the presence of many slightly different complement-like and EGF-like repeats, which may form multiple,

Reprint requests to: Peter G.W. Gettins, Department of Biochemistry and Molecular Biology, M/C 536, University of Illinois at Chicago, 1853 West Polk Street, Chicago, Illinois 60612-4316; e-mail: pgettins@tigger.cc.uic.edu.

Abbreviations: α_2M, α_2-macroglobulin; RBD, receptor binding domain; LRP, low density lipoprotein receptor-related protein; LDL, low density lipoprotein; VLDL, very low density lipoprotein; GSH, reduced glutathione; GSSG, oxidized glutathione; TOCSY, total correlation spectroscopy; HSQC, heteronuclear single quantum coherence; NOE, nuclear Overhauser enhancement; EGF, epidermal growth factor.

slightly different ligand binding sites. Although the exact location of the binding site of α_2M-proteinase complexes to LRP has not yet been determined, two studies have limited the region of interaction to the first multiple cluster of complement-like repeats, which is also the one most distant from the transmembrane region (Nielsen et al., 1995; Horn et al., 1997). These complement repeats are so named for their similarity to a cysteine-rich repeat found in complement components C8 and C9. Two NMR structures (Daly et al., 1995a, 1995b) and one crystal structure (Fass et al., 1997) of repeats from the related LDL receptor have been determined, and it has been proposed, based on the crystal structure of one such repeat with calcium bound, that familial hypercholesterolemia can result from mutations that adversely affect binding of calcium to the complement-like repeat and so reduce binding of the receptor to the α-helical, lysine-containing binding site of apolipoprotein E (Fass et al., 1997). The requirement for calcium also extends to the binding of α_2M-proteinase complexes to LRP (Moestrup et al., 1990).

In this study, we have used three-dimensional heteronuclear and multinuclear NMR methods to determine the secondary structure of recombinant human α_2M RBD to determine the nature of the structure that contains the critical lysine residues implicated in receptor binding.

Results

Preparation and characterization of recombinant RBD

The 165 residue $(His)_6$-tagged RBD fusion protein was expressed and purified as described in Materials and methods. It was found, however, that following refolding the protein was a mixture of monomeric and higher order species, as evidenced by bands of different mobility on PAGE under nondenaturing conditions, but only a single band when run on SDS-PAGE (not shown). This complexity was not resolved by digestion with thrombin to remove the polyhistidine tail. We therefore used papain cleavage to remove all residues that were not part of the core 138 residue RBD. This included not only the polyhistidine tag and thrombin cleavage site, but also the additional N-terminal α_2M residues that had been included to promote stability of the RBD (Holtet et al., 1994). Papain was used because this is the way RBD is normally prepared from plasma α_2M (Sottrup-Jensen et al., 1986). The resulting protein was monomeric and migrated as two bands on both reducing and nonreducing PAGE (Fig. 1). One band was unaffected by reduction, whereas the other changed mobility analogously to plasma-derived RBD. The two species were completely resolved by FPLC on MonoQ. The reduction-sensitive lower mobility species gave an N-terminal sequence of Glu-Glu-Phe-Pro-Phe and thus corresponded to full-length RBD with an intact disulfide. This was the species, whether unlabeled, ^{15}N-labeled, or $^{13}C/^{15}N$-labeled that was used for all further studies. The other species, which was not sensitive to reduction, gave an N-terminal sequence of Lys-Glu-Glu-Phe-Pro and thus corresponded to an alternative cleavage product that was one residue longer and that did not contain an intact disulfide. The shifted cleavage site presumably resulted from an altered fold connected with the absence of the disulfide. Plasma-derived RBD is normally a mixture of nonglycosylated (~10%) and glycosylated proteins, the latter carrying one carbohydrate chain at residue 1401. The nonglycosylated plasma-derived species migrated identically on SDS-PAGE to the correctly folded nonglycosylated recombinant RBD (not shown).

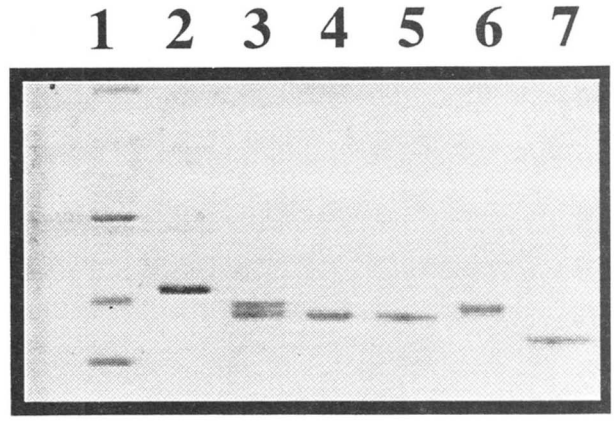

Fig. 1. Discrimination by 12% SDS-PAGE between correctly-folded and incorrectly-folded recombinant RBD obtained after cleavage of the larger construct by papain. Lane 1, low molecular weight markers (from bottom, lysozyme, trypsin inhibitor, carbonic anhydrase); lane 2, eluate from Ni-NTA column before removal of the N-terminal tail by papain cleavage, showing a single species under denaturing conditions; lane 3, RBD after cleavage by papain; lanes 4 and 5, incorrectly folded RBD without disulfide bond; lanes 6 and 7, correctly-folded protein with disulfide bond. Lanes 5 and 7 were run under nonreducing conditions; lanes 1–4 and 6 were run under reducing conditions. Only the RBD with an intact disulfide shows sensitivity of mobility to reduction (lanes 6 and 7).

The secondary structure of the recombinant RBD was compared with that of plasma-derived RBD by CD spectroscopy and shown to be very similar at the pH to be used for the NMR structural studies (pH 5.1) (Fig. 2). The CD spectrum of plasma RBD was

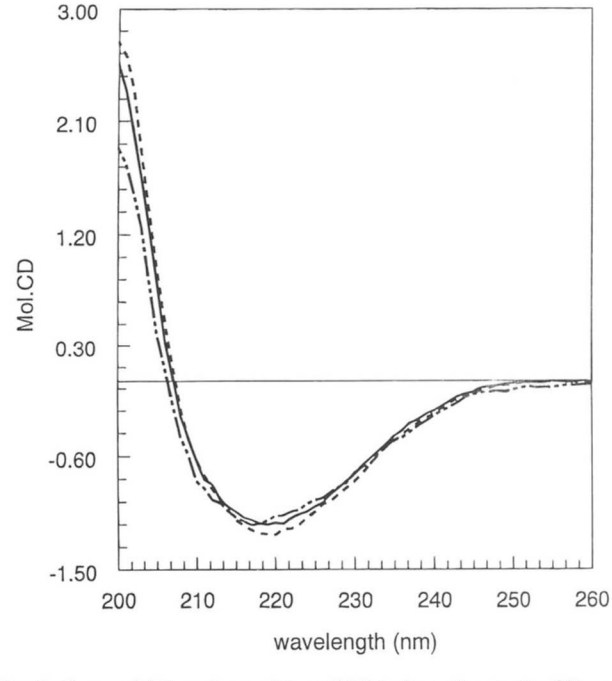

Fig. 2. Correct folding of recombinant RBD indicated by similar CD spectra for the plasma-derived and recombinant proteins. CD spectra of glycosylated plasma α2M-derived RBD at pH 5.1 (dashed line) and pH 7.4 (solid line) and of recombinant, nonglycosylated RBD at pH 5.1 (dot-dashed line).

also recorded at pH 7.4 and showed very little alteration from pH 5.1, indicating that the structure does not appear to be significantly pH-dependent in this pH range. One-dimensional ^{1}H NMR spectra in H_2O were also recorded for plasma-derived RBD and recombinant RBD at pH 5.1. Two regions of the spectra that are most sensitive to the fold of the protein are shown in Figure 3. These are the amide region, which shows backbone amide protons, and the most upfield region, which contains those resonances that are strongly upfield shifted, usually by proximity to one or more aromatic side chains. Both of these regions are typically very sensitive to small alterations in overall structure. The near identity of the two spectra agrees with the conclusion from the CD spectra that the fold of the recombinant protein is normal and also that the absence of the single carbohydrate chain from the recombinant protein has not perturbed the fold. The CD spectrum was also analyzed by the procedure of Manavalan and Johnson (1987) to obtain an estimate of the secondary structure content. This indicated that the domain was 28% β-sheet, 12% α-helix, and 23% β-turns.

CD was also used to determine the stability of the folded recombinant RBD under conditions to be used for the NMR experiments. In 0.1 M phosphate buffer, pH 5.1 containing 0.1 M NaCl the denaturation temperature was 70 °C. This was increased to 75 °C in the presence of an additional 0.3 M NaCl. NMR experiments were therefore carried out at higher salt to stabilize the protein for the long duration of the NMR experiments.

NMR secondary structure determination

A ^{1}H-^{15}N HSQC spectrum (Fig. 4) was initially run to confirm that the recombinant RBD was amenable to further conformational analysis by NMR. The spectrum showed good dispersion in both

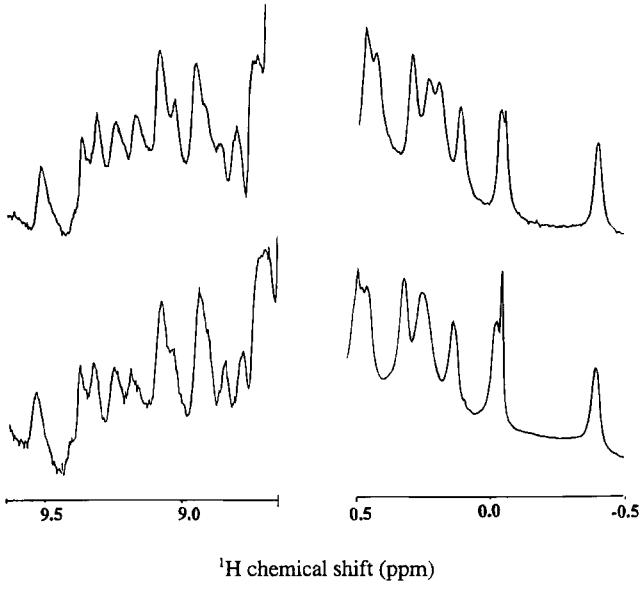

Fig. 3. Demonstration that nonglycosylated recombinant RBD and glycosylated plasma α_2M-derived RBD are structurally equivalent from the similarity of one-dimensional ^{1}H NMR spectra in structurally-sensitive regions; downfield amide region (left) and upfield region (right). Top spectrum, human plasma α_2M RBD; bottom spectrum, *E. coli* recombinant RBD. Both spectra were recorded at 600.13 MHz at pH 5.1 in H_2O.

^{1}H and ^{15}N dimensions, indicative of a compact globular protein and consistent with both the extensive secondary structure seen by CD spectroscopy and the very good dispersion in the aromatic and upfield regions of the ^{1}H NMR spectrum that indicated a hydrophobic core containing aromatic side chains. The resonance assignments shown in Figure 4 (Table 1) were made with the aid of both triple resonance experiments, and three-dimensional ^{15}N-edited NOESY and TOCSY spectra. Starting from distinctive residues such as glycine and alanine, small sequence elements were determined through sequential connectivities in triple resonance experiments. Experiments used in this work include an HNCA (Fig. 5), which displayed all assigned C_α resonances, an HNCACB and a CBCA(CO)NH. From these experiments the identity of individual amino acids was tentatively determined through characteristic C_α and C_β chemical shifts and then these small sequence elements were further assigned to areas in the protein by sequence comparisons. Some ambiguities in sequential connectivities of backbone C_α atoms were resolved on the basis of C_β chemical shift comparisons between the CBCA(CO)NH and HNCACB experiment. Sequential assignments were checked against both amide and side-chain NOE cross peaks in the event that C_β shifts were also degenerate or missing due to inefficient magnetization transfer. Finally, HBHA(CO)NH was used to obtain chemical shifts for proline H_α and H_β.

Both H_α and C_α chemical shifts were used to determine regions of defined secondary structure (Fig. 6). The chemical shift index (Wishart et al., 1992) is a quick and simple method to determine regions in the protein which are either α-helical or β-sheet in that C_α and H_α chemical shifts change in predictable ways relative to random coil. It is empirically found that the chemical shifts of C_α and H_α of amino acids involved in α-helices are shifted downfield and upfield, respectively whereas those in β-sheets are shifted in the opposite direction. The H_α chemical shift index showed that there are nine regions that are shifted downfield and one region shifted upfield, which indicated formation of nine strands of β-sheet and one region of α-helix, respectively (Fig. 6A). Eight of the regions of β-conformation and the region of α-helix were also seen from C_α chemical shift (Fig. 6B). The only discordance was for residues 52–54, which fulfilled the requirement for β-strand by H_α chemical shift index, but not by C_α chemical shift index. Since only one of these residues (Ile54) showed a strong negative ^{13}C chemical shift difference and since this residue is followed by a proline, it was considered less likely that this region is part of a β-sheet.

α-Helices and β-sheet structures also typically show characteristic NOE patterns (Wüthrich, 1986). For β-sheet structures, strong sequential $d_{\alpha N}$ and cross-strand d_{NN} and $d_{\alpha N}$ NOEs can be observed with only weak or nonexistent d_{NN} correlation. For α-helices, sequential correlations between amide protons, d_{NN} are expected, in addition to correlations from $d_{\alpha N}$ and $d_{\alpha N}(i, i + 3)$. Analysis of the NOE pattern again indicated that the secondary structure consisted of nine β-strands and one α-helix (Fig. 6C). Again, based on the discordance with the C_α ^{13}C chemical shift index for the region 52–54, it was considered that residues 52–54, though showing strong $d_{\alpha N}$ NOEs are not part of a β-sheet, though it may well be in an extended β-like conformation.

The consensus of the number and extent of the secondary structure elements was based on all three criteria presented above (^{1}H, ^{13}C, and NOE analyses) and is shown in each panel of Figure 6 as regions S1–S8 and H1. The eight β-sheet strands cover Phe5–Leu12 (S1), Thr23–Ser32 (S2), Met42–Val47 (S3), Arg71–Ser75

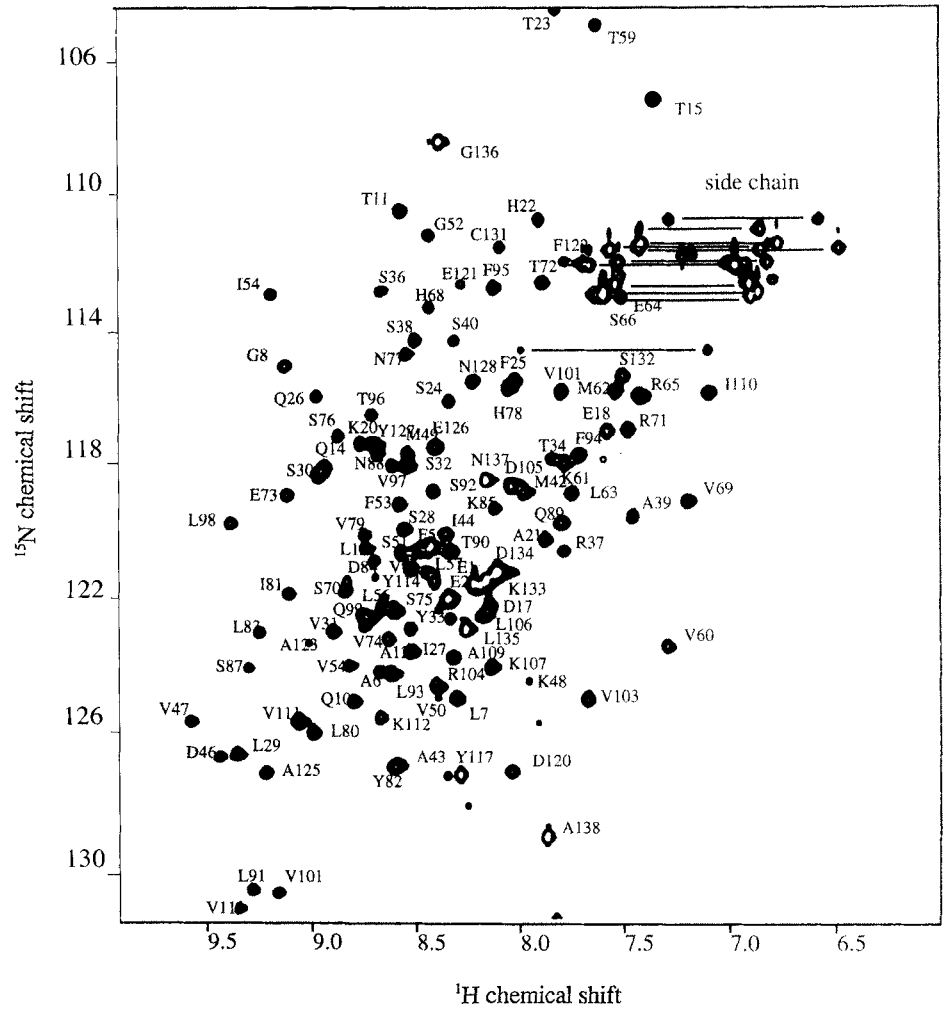

Fig. 4. ^{1}H-^{15}N GSE-HSQC spectrum of uniformly ^{15}N-labeled recombinant RBD. One cross peak is resolved for every backbone amide proton, except four nonproline residues, as labeled. Horizontal bars are drawn between pairs of related peaks that arise from side-chain amide NH_2 groups. All spectra presented in this paper were collected at 298 K, pH 5.1, and at 600.13 MHz proton frequency. The number of t1 complex points was 256 with a 153 ms acquisition time, and the number of complex points in t2 was 1024 with a 141 ms.

(S4), His78–Glu84 (S5), Leu91–Val97 (S6), Ala109–Lys112 (S7), and Ile124–Asn128 (S8), whereas the eight residue α-helix runs from Pro58–Arg65. Together the regions of α and β structure found experimentally covered 44% of the protein, which compares well with the amount of α/β obtained from analysis of the CD spectrum (40% α helix or β-strand).

The relationship of the eight strands in β-conformation to one another was determined from observed interstrand NOEs, both between amide proton and alpha carbon proton and between pairs of alpha carbon protons (Fig. 7). Three distinct regions of antiparallel β-sheet were identified, containing three, three, and two strands in β-conformation. The only α-helix begins at Pro58 as evidenced by the change in the C_α chemical shift and a $d_{\alpha N}$ NOE to Lys61. This helix lies between strands S3 and S4 in the primary structure, which are the outer two strands of a three-strand β-sheet. This can thus be considered to be a β-α-β unit with parallel β-strands and the helix in the crossover from the C-terminal end of the first strand to the N-terminal of the second strand, though with an intervening third β-strand (S5) to give an overall antiparallel β-sheet.

Secondary structure was also predicted by the method of Rost and Sander (1993a, 1993b, 1994) both for human α_2M RBD and for the equivalent regions of other α-macroglobulins (Fig. 8). The predictions for all eight α-macroglobulins were very similar, with seven regions in β-conformation and one α-helix being common to all. The major difference was for a second α-helix at the C-terminal end. This was absent in PZP and merged with a small region in β-conformation in others. For none of the proteins was the numerical prediction of α-helix strong in this C-terminal region. The consensus was thus for seven strands in β-conformation and one α-helix. All of these were found in the NMR structure, though the lengths of strands S3, S6, and S7 were significantly shorter and of S1 longer than predicted and the α-helix was longer than predicted. The eighth β-strand found by NMR (S8) corresponded to the region of nonconsistent prediction of α/β close to the C-terminus and covered the end predicted more consistently to be in β conformation. The total prediction of α and β structure was 8% and 63%, which was considerably higher than found here from the NMR secondary structure or from analysis of the CD spectrum.

Table 1. *Chemical shifts assignments for most of backbone amide nitrogen and proton, and C_α carbon and proton*

Residue	^{15}N	^{1}H-N	$^{13}C_\alpha$	$^{1}H_\alpha$	Residue	^{15}N	^{1}H-N	$^{13}C_\alpha$	$^{1}H_\alpha$
1E	121.3	8.28	56.0	4.17	70S	121.8	8.89	59.0	4.37
2E	121.5	8.37	56.0	4.20	71R	116.9	7.51	55.6	4.33
3F	121.3	8.28	56.4	4.44	72T	112.5	7.94	59.5	5.31
4P			62.9	4.71	73E	118.9	9.17	55.3	4.66
5F	120.4	8.46	56.6	5.05	74V	122.8	8.81	61.6	4.59
6A	124.2	8.73	50.9	4.49	75S	122.3	8.64	56.3	4.79
7L	125.0	8.36	53.0	5.25	76S	116.1	8.92	60.4	4.66
8G	115.1	9.17	44.7	4.57, 3.59	77N	114.7	8.59	53.2	4.73
9V	120.7	8.57	60.2	4.92	78H	115.7	8.09	54.8	5.46
10Q	125.1	8.84	53.6	4.79	79V	120.2	8.79	61.5	4.41
11T	110.4	8.62	59.7	5.34	80L	126.0	9.03	53.2	5.39
12L	120.5	8.79	51.9	4.64	81I	121.9	9.15	60.6	4.19
13P			63.3	4.89	82Y	127.1	8.66	57.4	4.63
14Q	118.1	8.99	57.7	4.05	83L	123.0	9.29	52.4	5.43
15T	107.0	7.39	59.0	4.52	84D	120.8	8.74	53.7	4.75
16C	120.6	8.51	56.1	4.69	85K	119.3	8.17	56.9	3.88
17D	122.2	8.18	54.9	4.46	86V	122.6	8.38	62.6	3.89
18E	117.1	7.61	53.6	4.82	87S	124.1	9.31	56.5	5.02
19P			65.9	4.31	88N	117.6	8.72	54.6	4.71
20K	117.4	8.8	58.6	4.25	89Q	119.8	7.84	55.2	4.29
21A	120.3	7.91	53.9	4.58	90T	120.6	8.37	64.4	4.03
22H	110.6	7.95	58.3	4.17	91L	130.8	9.32	53.7	4.56
23T	104.4	7.86	61.6	4.56	92S	118.8	8.46	56.7	5.41
24S	116.1	8.39	58.2	5.22	93L	124.2	8.66	53.3	4.74
25F	115.4	8.06	56.6	4.98	94F	117.7	7.77	55.5	5.93
26Q	115.1	9.01	53.9	5.13	95F	112.7	8.17	57.5	4.87
27I	123.6	8.57	60.9	3.84	96T	114.5	8.75	63.1	4.73
28S	120.0	8.6	55.2	4.93	97V	118.1	8.66	58.8	5.01
29L	126.6	9.41	53.1	5.15	98L	119.8	9.43	53.2	5.20
30S	118.3	9.01	56.4	5.41	99Q	122.5	8.78	56.5	5.64
31V	122.9	8.94	60.0	5.31	100D	130.9	9.2	55.0	4.69
32S	117.4	8.58	57.5	4.62	101V	115.8	7.83	58.3	4.46
33Y	123.1	8.54	57.2	4.70	102P			62.3	4.17
34T	117.8	7.9	60.2	4.12	103V	125.1	7.71	61.5	4.09
35G	107.6	5.16	44.8	3.32, 4.04	104R	124.6	8.45	57.3	4.19
36S	112.9	8.71	59.5	4.23	105D	118.7	8.09	53.2	4.62
37R	120.5	7.86	56.1	4.45	106L	122.5	8.22	54.8	4.26
38S	114.3	8.54	60.9	4.11	107K	124.0	8.18	53.6	4.59
39A	119.6	7.51	51.3	4.18	108P			62.7	4.26
40S	114.3	8.37	57.6	3.99	109A	123.8	8.36	49.7	4.60
41N	121.8	8.38	54.5	4.71	110I	115.8	7.14	59.8	4.77
42M	118.8	8.05	56.6	4.88	111V	125.6	9.11	60.4	4.93
43A	126.9	8.63	50.1	5.01	112K	125.7	8.71	53.8	5.45
44I	120.0	8.41	56.2	4.26	113V	122.5	8.79	57.5	5.67
45V	124.1	8.87	60.2	4.47	114Y	121.4	8.37	56.9	4.21
46D	126.8	9.49	51.9	5.24	115D	121.5	8.7	52.9	3.86
47V	125.7	9.63	61.1	4.28	116Y	122.1	8.19	61.1	4.67
48K	124.4	8.32	52.7	4.56	117Y	127.3	8.32	52.7	4.57
49M	122.2	8.37	54.2	4.41	118E	120.6	8.39	56.0	4.76
50V	125.0	8.43	62.7	3.84	119T	113.2	8.17	61.2	4.03
51S	120.7	8.62	60.5	4.21	120D	127.2	8.07	55.5	4.41
52G	111.1	8.48	45.7	4.41, 3.81	121E	112.6	8.31	56.0	3.76
53F	119.2	8.62	57.5	5.15	122F	111.9	7.84	59.0	4.82
54I	112.9	9.24	57.4	4.99	123A	123.4	9.06	50.8	4.29
55P			62.1	4.75	124I	120.3	8.54	59.3	5.38
56L	122.2	8.71	53.7	4.14	125A	127.2	9.27	51.4	4.69
57K	121.5	8.45	55.0	4.98	126E	117.4	8.45	54.4	5.47
58P			66.2	4.41	127Y	117.5	8.75	55.9	4.75
59T	104.8	7.66	64.1	4.41	128N	115.5	8.27	50.1	4.62
60V	123.4	7.31	65.1	3.50	129A	123.6	8.67	50.0	3.30
61K	118.0	7.81	57.6	3.91	130P			64.3	3.97
62M	115.8	7.57	57.8	4.13	131C	111.5	8.14	54.3	4.70
63L	118.8	7.78	57.1	4.09	132S	115.3	7.53	59.9	4.16
64E	113.0	7.55	57.7	3.76	133K	121.4	8.15	55.9	
65R	115.9	7.46	57.4	4.13	134D	121.4	8.15	54.2	4.57
66S	112.9	7.67	57.9	4.42	135L	122.5	8.29	55.3	4.27
67N	125.7	9.09	54.9	4.46	136G	108.3	8.42	45.4	3.88
68H	113.2	8.48	56.4	4.66	137N	118.4	8.2	53.0	4.70
69V	119.1	7.25	60.9	4.64	138A	129.1	7.9	53.8	4.05

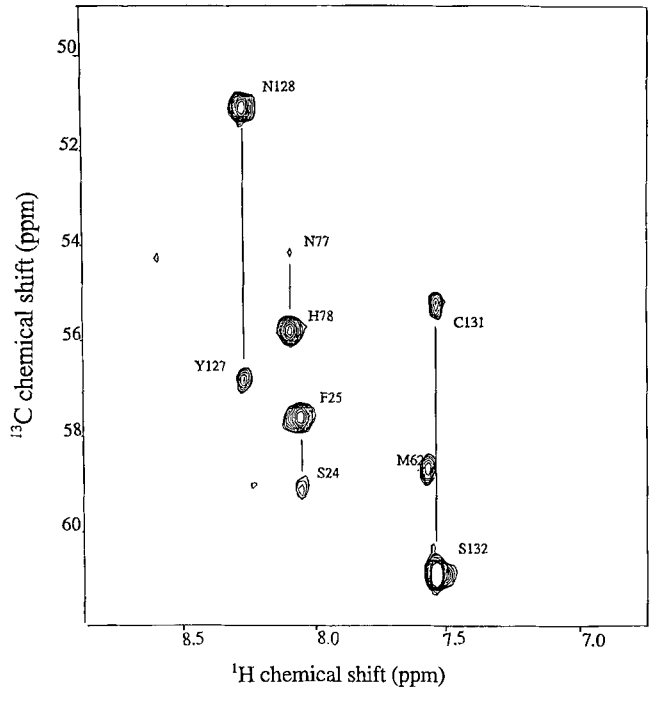

Fig. 5. HNCA spectrum of uniformly ^{15}N and ^{13}C labeled recombinant RBD at ^{15}N chemical shift of 115.76 ppm. The data were collected as a 120 × 32 × 512 complex matrix with acquisition times of t1 (^{13}C) = 23.5 ms, t2 (^{15}N) = 21.3 ms, and t3 (^{1}H) = 61.4 ms.

However, there was overall excellent agreement between prediction and experiment in the number and location of secondary structure elements and an apparently very similar structure for this domain in all of the sequences of α-macroglobulins examined.

Discussion

Human α_2M binds to its receptor LRP only after proteinase-induced conformational changes have occurred in the α_2M. However, since the 138 residue C-terminal domain retains high affinity for LRP when isolated from α_2M (Sottrup-Jensen et al., 1986), it is likely that the receptor binding epitope of α_2M already exists in the native protein and is a part of the discrete RBD. Isolated RBD is therefore likely to be a good model for understanding the binding of α_2M-proteinase complexes to LRP. Site-directed mutagenesis has implicated two lysine residues (1370 and 1374) as part of the receptor-binding epitope in RBD. In the present study we have used NMR spectroscopy to show that RBD is a well-structured globular protein with extensive β-sheet secondary structure, and most importantly, that the two lysine residues that are critical for receptor binding are located in or immediately adjacent to the single α-helix of the domain, which is part of a $\beta\alpha\beta$ unit and may lie on top of a three-strand β-sheet. Such a motif of basic residues in an α-helical region has been seen with other protein ligands of receptors that belong to the LDL receptor family, such as LRP, and may be a common feature of binding of these receptors to their protein ligands.

Based both on earlier chemical modification results that implicated lysine residues in binding of RBD to the receptor (Sottrup-Jensen et al., 1986) and on identification of residues that are conserved in the equivalent domain of other α-macroglobulins, Nielsen et al. (1996) carried out mutagenesis of five of the eight lysine residues present in RBD (1333, 1361, 1370, 1374, and 1425). Mutation of lysines 1333, 1361, or 1425 produced no detectable alteration in binding to receptor. Mutation of either Lys1370 or Lys1374, however, gave a 10–50-fold reduction in affinity, thus implicating both in high affinity binding of RBD to the receptor. Our present study shows that, in addition to Lys1370 being close to Lys1374 as a result of two of the intervening residues being part of an α-helix, another basic residue, Arg1378, should be adjacent to Lys1374 since it is also part of the α-helix and should be on the same face of the helix as Lys1374. These three basic residues are therefore likely to constitute a patch of positive charge along the outer face of the helix and may collectively form a major part of the binding site for the receptor.

If the receptor binding region of RBD is composed of positively charged residues presented on the side of an α-helix, it might be expected that other α-macroglobulins that bind to LRP would contain a similar structure. This is supported by our secondary structure predictions of seven other α-macroglobulins. All show a strong prediction of α-helix in this region very similar to the prediction for human α_2M. In addition, all known sequences of α-macroglobulins from mammalian sources contain lysines at positions equivalent to Lys1370 and Lys1374 of human α_2M, as well as either arginine at position 1378 or an additional lysine at position 1375.

A binding motif for human α_2M to RBD of two or three positively charged residues on one face of an α-helix is also in keeping both with the structures of three complement-like domains from the LDL receptor (Daly et al., 1995a, 1995b; Fass et al., 1997) and with the proposed binding mode of apolipoprotein E to the LDL receptor and to LRP (Wilson et al., 1991). The complement-like repeats in the LDL receptor family of proteins are about 40–45 residues long and fold with three disulfides into an elongated structure of long axis about 30 Å. Each repeat contains a high proportion of negatively charged residues, mostly 8 to 10. Of these negative residues four appear to be required for Ca^{2+} binding and are buried in the calcium complex (Fass et al., 1997). This leaves, however, up to six surface negative charges that are available for interaction with basic residues on protein ligands. In repeat five of the LDL receptor, four of these negative residues are on one face and extend along the long axis of the domain. This would be an appropriate surface to interact with basic residues along an α-helix of as many as five turns. In the case of apoliprotein E, it has been proposed, based on reduced receptor affinity of naturally occurring variants of this repeat, that eight basic residues in just such a five turn stretch of α-helix are responsible for binding to the receptor (Wilson et al., 1991). Since no single mutation abolishes binding, it was suggested that there are multiple charged interactions that contribute to the overall binding energy. Both repeat one and repeat two of the LDL receptor also have similarly arrayed stretches of negatively charged residues along the long axis of the domain that could interact with extended α-helical regions containing basic residues along one face. In the case of α_2M, the much shorter extent of the α-helix and the fewer basic residues present make it likely that the helix makes contact with only some of the negatively charged groups. However, to account for the high affinity of RBD for the receptor (~50 nM for the isolated domain), it is likely that there are additional nonpolar interactions that contribute to the binding energy. In this regard it may be significant that there is a strong pH-dependence of binding of both α_2M and LDL to their receptors. It is reported that binding falls dramatically below pH 6.8 (Basu et al., 1978; Maxfield, 1982). It seems unlikely that such

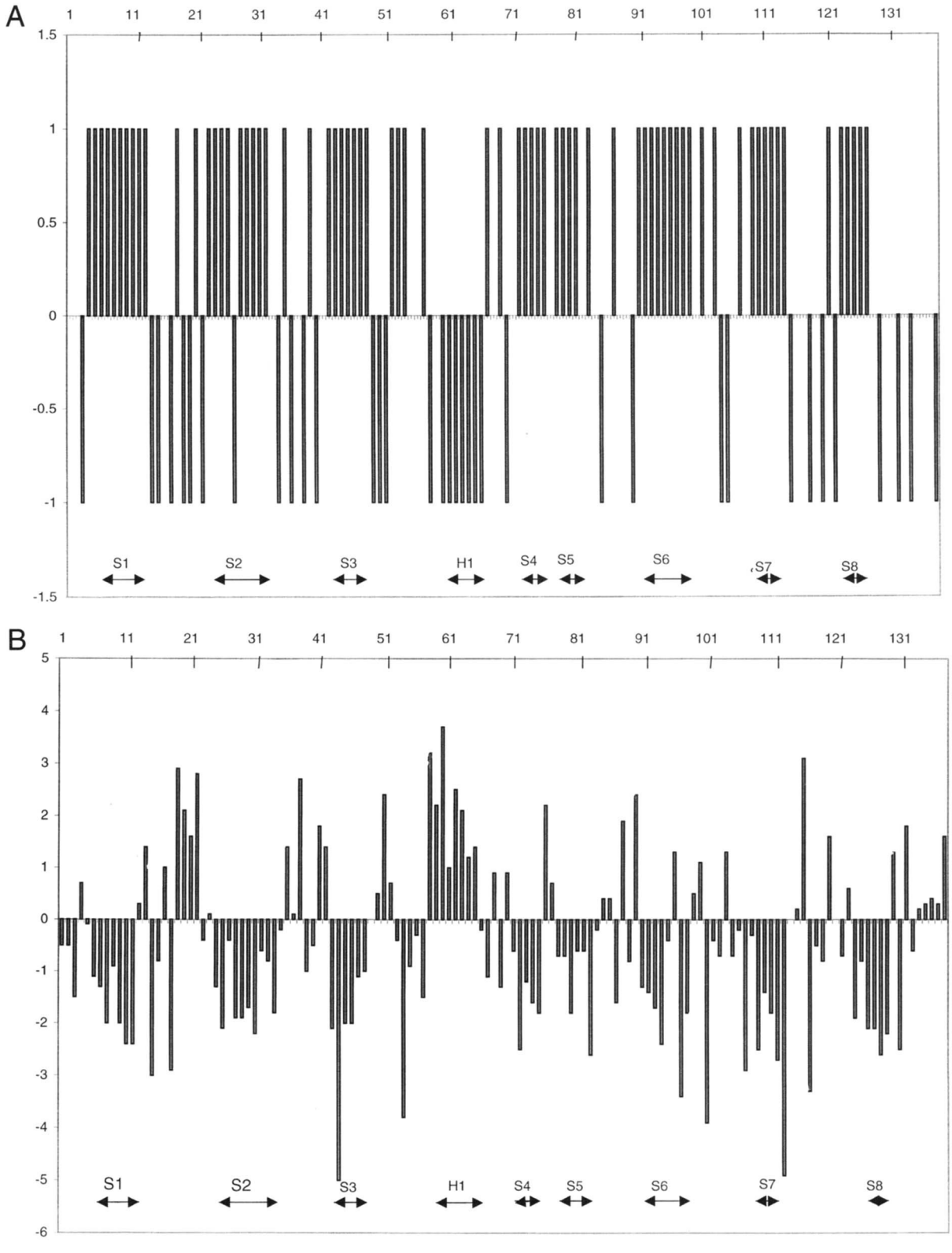

Fig. 6. Determination of number and extent of regions of secondary structure using chemical shift indices and intrastrand NOEs. The consensus regions of β-sheet and α-helix are indicated using the designations S1–S8 and H1. **A:** H_α chemical shift index plot of recombinant RBD. The chemical shift index is given the value -1 if the chemical shift is less than random coil range, 0 if it is within the random coil range, and $+1$ if it is higher than the random coil range. Any "dense" grouping of four or more "-1 s" not interrupted by a "$+1$" is a helix. Any dense grouping of three or more "$+1$s" not interrupted by "-1" is a β-strand. **B:** C_α chemical shift index plot of RBD. The values plotted are the difference in ^{13}C chemical shift from the corresponding random coil chemical shifts. **C:** Regions of secondary structure indicated by NOEs. Thick lines indicate strong NOEs, thin lines represent weak NOEs. (*Figure continues on facing page.*)

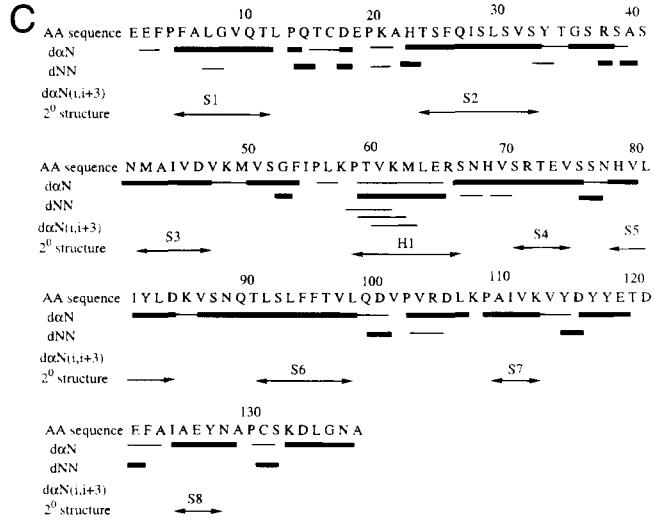

Fig. 6. *Continued.*

a pH-dependence could arise from protonation of carboxyl groups, either ones that are ligands for the calcium ions in the receptor or involved in charged interactions with α_2M. The more likely basis for such a pH-dependence is protonation of histidine. In human α_2M RBD histidine occurs two residues C-terminal to the α-helix and may thus also form part of the binding site for LRP. In apolipoprotein E one of the residues in the basic cluster that is proposed to be the binding site for receptor is also a histidine.

Materials and methods

Construction of the RBD expression plasmid

The α_2M expression plasmid p1167 (a gift from Dr. Esper Boel) was digested with *Sac*I to give four fragments of size 6.1, 1.2, 0.86, and 0.55 kb. The 1.2 kb fragment, which spanned from base 4642 to base 5868 and covered the sequence coding for the receptor binding domain, was purified and ligated into the mutagenesis plasmid pAlter1 (Promega) that had been cut with *Sac*I. Using the Altered sites II mutagenesis kit and the manufacturer's protocol, an *Nde*I restriction site was created at position 5368 by change of the sequence CAGACA to CATATG. A subsequent round of mutagenesis was used to create a *Bam*HI site at position 5830 by change of the sequence from GGCTGA to GGATCC. The 460 base *Nde*I–*Bam*HI fragment was excised and ligated into the commercial expression vector pET15b (Novagen, Madison, Wisconsin) between the *Nde*I and *Bam*HI sites. This gave a construct that expressed a 165 residue protein with the sequence/structure of $(His)_6$Ser-Ser-Gly-Leu-Val-Pro-Arg-Gly-Ser-His-Met-^{1304}Ser--------^{1451}Ala^2. The underlined dipeptide is a thrombin cleavage site, $(His)_6$ is a polyhistidine tag for subsequent purification, and the sequence ^{1304}Ser--------^{1451}Ala represents the 148 residue portion of human α_2M that covers the receptor binding domain (^{1314}Glu–^{1451}Ala) as well as an additional 10 residues N-terminal that were originally thought to be necessary for increased stability (Holtet et al., 1994).

Expression and purification of unlabeled and isotopically-enriched recombinant RBD

The 165 residue fusion protein was expressed in *Escherichia coli* transformed with the pET15b-RBD fusion construct by induction of T7 polymerase at mid-log growth, through the addition of 1 mM IPTG. Uniformly labeled RBD was grown in isotopically enriched minimal medium containing 0.6% Na_2HPO_4, 0.3% KH_2PO_4, 0.15% NaCl, 0.6% Basal Medium Eagle Vitamin Solution (Gibco), and mineral element supplement. 1 g/L $(^{15}NH_4)_2SO_4$ and 2 g/L of unlabeled glucose were used for ^{15}N labeling and 1.2 g/L $(^{15}NH_4)_2SO_4$ and 2 g/L of ^{13}C glucose for double labeling. Protein expression was induced at an OD_{600} of 0.5 and cells were grown for a further 14–18 h at 37 °C before being harvested by centrifugation. Cells were lysed by sonication. Inclusion bodies were harvested by centrifugation and dissolved in 0.1 M Na_2HPO_4, 0.01 M Tris buffer pH 8.0 containing 10 mM β-mercaptoethanol. The protein was purified by affinity chromatography on an Ni-NTA column (Qiagen, Santa Clarita, California) under denaturing conditions using the manufacturer's protocol.

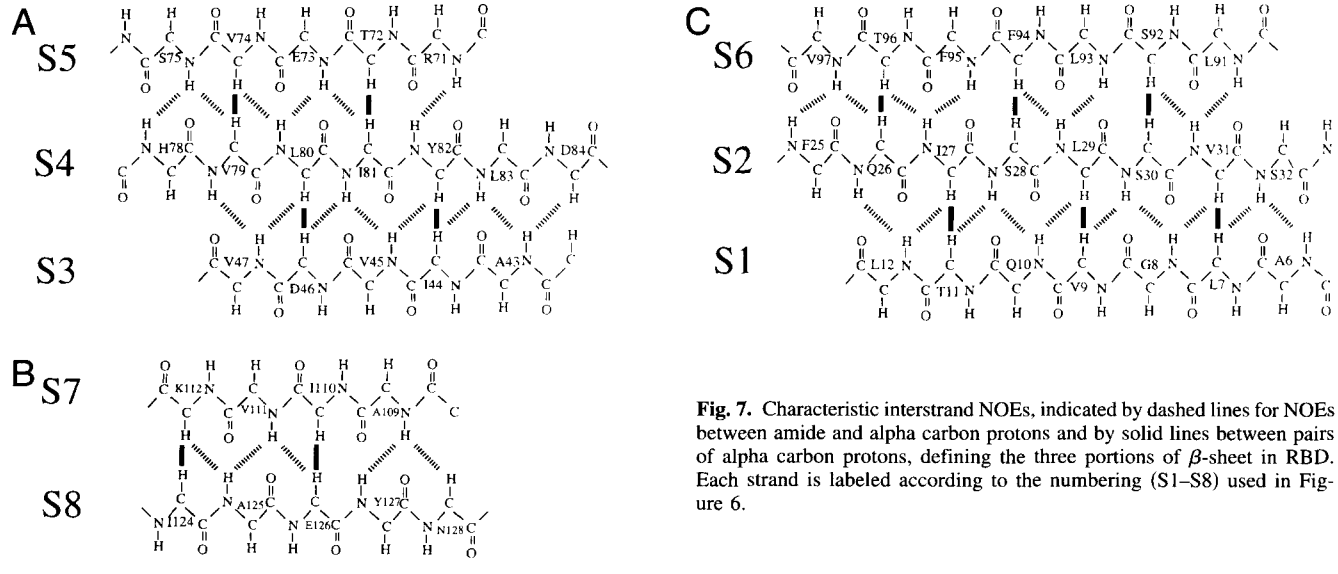

Fig. 7. Characteristic interstrand NOEs, indicated by dashed lines for NOEs between amide and alpha carbon protons and by solid lines between pairs of alpha carbon protons, defining the three portions of β-sheet in RBD. Each strand is labeled according to the numbering (S1–S8) used in Figure 6.

AA sequence	E	E	F	P	F	A	L	G	V	Q	T	L	P	Q	T	C	D	E	P	K	A	H	T	S	F	Q	I	S	L	S
NMR 2° structure					β-sheet (S1)																			β-sheet (S2)						
Human α2M					S	S	S	S	S	S														S	S	S	S	S	S	S
Human PZP					S	S	S	S	S	S													S	S	S	S	S	S	S	S
Rat α1M					S	S	S	S	S															S	S	S	S	S	S	S
Mug1					S	S	S	S	S	S														S	S	S	S	S	S	S
Mouse α2M					S	S	S	S	S	S															S	S	S	S	S	S
Rat α1I3					S	S	S	S	S	S														S	S	S	S	S	S	S
Limulus α2M					S	S	S	S	S	S														S	S	S	S	S	S	S
Bovine α2M					S	S	S	S	S	S														S	S	S	S	S	S	S

AA sequence	V	S	Y	T	G	S	R	S	A	S	N	M	A	I	V	D	V	K	M	V	S	G	F	I	P	L	K	P	T	V
NMR 2° structure												β-sheet (S3)																	α-helix		
Human A2M	S	S	S	S								S	S	S	S	S	S	S	S	S	S	S						H	H	
Human PZP	S	S	S	S								S	S	S	S	S	S	S	S	S	S	S	S						H	
Rat α1M	S	S	S	S								S	S	S	S	S	S	S	S	S	S	S	S						H	
Mug 1	S	S	S	S								S	S	S	S	S	S	S	S	S	S	S							H	
Mouse α2M	S	S	S	S								S	S	S	S	S	S	S	S	S	S	S	S					H	H	
Rat α1I3	S	S	S	S								S	S	S	S	S	S	S	S	S	S	S	S						H	
Limulus α2M	S	S	S	S								S	S	S	S	S	S	S	S	S	S	S	S						H	
Bovine α2M	S	S	S	S								S	S	S	S	S	S	S	S	S	S	S	S					H	H	

AA sequence	K	M	L	E	R	S	N	H	V	S	R	T	E	V	S	S	N	H	V	L	I	Y	L	D	K	V	S	N	Q	T
NMR 2° structure	α-helix(H1)										β-sheet (S4)								β-sheet (S5)											
Human α2M	H	H	H	H					S	S	S	S	S	S					S	S	S	S	S	S	S					
Human PZP	H	H	H						S	S	S	S	S	S					S	S	S	S	S	S	S	S			S	S
Rat α1M	H	H	H							S	S	S	S	S					S	S	S	S	S	S						S
Mug1	H	H	H							S	S	S	S	S					S	S	S	S	S	S						S
Mouse α2M	H	H	H	H						S	S	S	S	S					S	S	S	S	S	S					S	S
Rat α1I3	H	H	H	H					S	S	S	S	S	S					S	S	S	S	S	S	S				S	S
Limulus α2M	H	H	H	H					S	S	S	S	S	S	S				S	S	S	S	S	S						
Bovine α2M	H	H	H	H					S	S	S	S	S	S						S	S	S	S	S	S					S

AA sequence	L	S	L	F	F	T	V	L	Q	D	V	P	V	R	D	L	K	P	A	I	V	K	V	Y	D	Y	Y	E	T	D
NMR 2° structure	β-sheet (S6)																		β-sheet (S7)											
Human A2M	S	S	S	S	S	S	S	S	S	S	S	S							S	S	S	S	S	S	S					
Human PZP	S	S	S	S	S	S	S	S	S	S	S	S	S						S	S	S	S	S	S	S					
Rat α1M	S	S	S	S	S	S	S	S	S										S	S	S	S	S	S						H
Mug1	S	S	S	S	S	S	S	S	S	S	S	S	S						S	S	S	S	S	S						
Mouse α1M	S	S	S	S	S	S	S	S	S	S	S								S	S	S	S	S	S	S					H
Rat α1I3	S	S	S	S	S	S	S	S	S	S	S	S							S	S	S	S	S	S						
Limulus α2M	S	S	S	S	S	S	S	S	S	S									S	S	S	S	S	S					H	H
Bovine α2M	S	S	S	S	S	S	S	S	S	S	S								S	S	S	S	S	S						H

AA sequence	E	F	A	I	A	E	Y	N	A	P	C	S	K	D	L	G	N	A
NMR 2° structure			β-sheet (S8)															
Human A2M	H	H	H	H	H	S	S											
Human PZP			S	S	S	S	S											
Rat α1M	H	H	H	H	H	S	S											
Mug1	H	H	H	H	H	S	S											
Mouse α2M	H	H	H	H	H	H	S											
Rat α1I3	H	H	H	H	S	S	S	S										
Limulus α2M	H	H	H	H	H	H												
Bovine α2M	H	H	H	H	H	S	S											

Fig. 8. Comparison of NMR-determined consensus secondary structure with predicted secondary structure for human α_2M RBD and equivalent region of other α-macroglobulins. The amino acid sequence given is for human α_2M. The heavy lines indicate regions of secondary structure for human RBD determined here by NMR spectroscopy. The letter "S" indicates prediction of β conformation and the letter "H" prediction of α-helical conformation by the procedure of Rost and Sander.

The fusion protein was refolded while immobilized on the Ni-NTA column by washing for 8 h with 50 mM Tris buffer pH 8.0 containing 500 mM NaCl, 10% glycerol, and 3 mM β-mercaptoethanol. RBD fusion protein was eluted from the Ni-NTA column with 500 mM NaCl, 50 mM Tris, 20 mM EDTA, pH 8.0, and dialyzed against 500 mM NaCl, 50 mM Tris, 3 mM GSH, and 0.3 mM GSSG to form the disulfide bond. The N-terminal fusion tail, containing the $(His)_6$ linker, the thrombin cleavage site and the extra 10 α_2M residues that we originally believed were necessary for optimal stability and refolding, was removed by cleavage at room temperature for 3 h with 1/100 (w/w) papain (Boehringer Mannheim) in 0.1 M sodium acetate buffer, pH 4.5, containing 5 mM cysteine to activate the papain. Reduced SDS-PAGE showed two bands after papain cleavage (Fig. 1), the upper of which was subsequently shown to be correctly folded and disulfide-linked 138 residue RBD. RBD was isolated by ion-exchange chromatography on Mono Q (Pharmacia), using a linear gradient from 0 to 300 mM NaCl in 20 mM Tris, pH8.0. RBD eluted at 160 mM NaCl.

N-terminal sequence analysis was carried out by Edman degradation on an ABS 477A sequencer (Applied Biosystems). PTH-amino acid derivatives were quantitatively transferred to an ABI 120A HPLC system containing a PTH C-18 reverse-phase Brownlee column eluted with a sodium acetate buffer/acetonitrile gradient and identified at 269 nM.

CD spectroscopy

CD spectra were recorded in a 1 mm cell at room temperature on a JASCO 710 spectropolarimeter. The region from 200–260 nM was recorded, with scan rate of 2 nM min^{-1}, and response time of 16 s. The instrument was calibrated prior to each set of runs with a standard of 0.06% ammonium camphor. Filtered and degassed protein samples were in 50 mM sodium phosphate buffer and had concentrations of 0.5 mg/mL. Secondary structure analysis of the spectra was carried out using the variable selection program (Manavalan & Johnson, 1987) with a basis set of 18 of the proteins provided with the program.

The thermal stability of the 138 residue RBD was determined by monitoring the CD signal at 222 nM as a function of temperature, with an 8 s response time and a 2 nM band width. A jacked 1 mm cell was heated at 0.5 °C/min and data were collected at intervals of 0.5 °C. Each temperature scan was repeated two times.

NMR spectroscopy

NMR spectra were recorded at 600 MHz for ^1H either on a Bruker DRX600 at the University of Illinois at Chicago, or a Bruker DMX600 at the University of Wisconsin, Madison. Both instruments were equipped with three channels and a pulsed-field-gradient accessory. NMR data were processed and analyzed using Triad 6.2 software (Tripos, Inc., St. Louis, Missouri).

Purified RBD was exchanged into NMR buffer (100 mM phosphate, pH 5.1, 300 mM NaCl), to which 10% D_2O was added. The high salt concentration was used to maintain solubility of the protein at the high concentrations used for the NMR studies, but did not affect the structure of the protein, as judged by similarity of NMR and CD spectra under high and low salt conditions. The final concentration for NMR studies was 0.9 mM for the ^{15}N-labeled sample and 1.2 mM for the $^{13}C/^{15}N$ double labeled sample.

The following experiments were recorded on RBD at 298 K with either ^{15}N or $^{13}C/^{15}N$ labeled samples; two-dimensional ^{15}N-HSQC, three-dimensional ^1H-^{15}N-edited TOCSY and NOESY-HSQC(Fesik & Zuiderweg, 1990). Triple resonance experiments HNCA (Kay et al., 1990), HNCACB (Wittekind & Müller, 1993), and CBCA(CO)NH (Grzesiek & Bax, 1992) were also recorded for sequential assignment purposes. The proline H_α and H_β chemical shifts were identified from the HBHA(CO)NH experiment (Grzesiek & Bax, 1993). The center frequencies for these triple resonance experiments were 4.74 ppm (^1H), 118 ppm (^{15}N), 43 ppm (^{13}C) (CAB), and 55 ppm (^{13}C) (CA). Sensitivity enhancement gradient pulses were employed for experiments where magnetization was detected on the amide HN (Palmer et al., 1991; Muhandiram & Kay, 1994). ^1H, ^{13}C, and ^{15}N assignments for the backbone of RBD have been deposited with the BioMagResBank data base (http://www.bmrb.wisc.edu) with accession number BMRB-653.

Secondary structure predictions

Secondary structure predictions used the neural training network method developed by Rost and Sander (1993a, 1993b, 1994). This method uses three levels of evaluation, with the third level being a winner-takes-all prediction of helix, strand or loop secondary structure. For water soluble proteins this has been found to give prediction of secondary structure to an accuracy of better than 70% (Rost & Sander, 1993a). Sequences for analysis were submitted electronically to EMBL (http://www.embl-heidelberg.de/predictprotein/predictprotein.html) (Rost et al., 1994).

Materials

Oligonucleotides and enzymes were from Gibco BRL. $(^{15}NH_4)_2SO_4$ was from Cambridge Isotopes (Andover, Massachusetts), ^{13}C glucose was from Isotec (Miamisburg, Ohio), and D_2O was from Sigma (St. Louis, Missouri). Papain was from Boehringer Mannheim and gave specific cleavage, in contrast to papain from Sigma, which gave additional cleavages.

Acknowledgments

We thank Dr. Esper Boel for the generous gift of the α_2M expression plasmid p1167, Dr. Bingqi Fan for construction of the RBD expression plasmid, and Dr. Ian Marsden for help with some of the early NMR experiments. The Bruker DRX600 was purchased with funds from the University of Illinois at Chicago, and a grant from the NSF Academic Research Infrastructure Program (BIR-9601705). The DMX600 at the University of Wisconsin at Madison is supported by NIH grant RR02301 from the Biomedical Research Technology Program, and contains equipment purchased with funds from the University of Wisconsin, the NSF Biological Instrumentation Program (DMB-8415048), the NSF Academic Research Infrastructure Program (BIR-9214394), the NIH Biomedical Research Technology Program (RR02301), the NIH Shared Instrumentation Program (RR02781), and the U.S. Department of Agriculture. N-terminal sequence determination was carried out by Dr. Bob Lee in the Protein Sequencing Facility at the University of Illinois at Chicago. This work was supported by NIH grant GM54414 (P.G.W.G.). K.D. was supported by a postdoctoral fellowship from the Danish Natural Science Research Council. X.L. is the recipient of a Junior Faculty Award from the American Cancer Society.

References

Barrett AJ, Brown MA, Sayers CA. 1979. The electrophoretically "slow" and "fast" forms of the α_2-macroglobulin molecule. *Biochem J 181*:401–418.

Barrett AJ, Starkey PM. 1973. The interaction of α_2-macroglobulin with proteinases. Characteristics and specificity of the reaction and a hypothesis concerning its molecular mechanism. *Biochem J 133*:709–724.

Basu SK, Goldstein JL, Brown MS. 1978. Characterization of the low density lipoprotein receptor in membranes prepared from human fibroblasts. *J Biol Chem 253*:3852–3856.

Daly NL, Djordjevic JT, Kroon PA, Smith R. 1995a. Three-dimensional structure of the second cysteine-rich repeat from the human low-density lipoprotein receptor. *Biochemistry 34*:14474–14481.

Daly NL, Scanlon MJ, Djordjevic JT, Kroon PA, Smith R. 1995b. Three-dimensional structure of a cysteine-rich repeat from the low-density lipoprotein receptor. *Proc Natl Acad Sci USA 92*:6334–6338.

Fass D, Blacklow S, Kim PS, Berger JM. 1997. Molecular basis of familial hypercholesterolaemia from structure of LDL receptor module. *Nature 388*:691–693.

Fesik SW, Zuiderweg ERP. 1990. Heteronuclear 3-dimensional NMR spectroscopy of isotopically labeled biological macromolecules. *Q Rev Biophys 23*:97–131.

Grzesiek S, Bax A. 1992. Correlating backbone amide and side-chain resonances in larger proteins by multiple relayed triple resonance NMR. *J Am Chem Soc 114*:6291–6293.

Grzesiek S, Bax A. 1993. Amino acid type determination in the sequential assignment procedure of uniformly labeled $^{13}C/^{15}N$ enriched proteins. *J Biomol NMR 3*:185–204.

Hanover JA, Rudick JE, Willingham MC, Pastan I. 1983. α_2-Macroglobulin binding to cultured fibroblasts: Identification by affinity chromatography of high affinity binding sites. *Arch Biochem Biophys 227*:570–579.

Herz J, Hamann U, Rogne S, Myklebost O, Gausepohl H, Stanley KK. 1988. Surface location and high calcium affinity of a 500 kD liver membrane protein closely related to the LDL-receptor suggest a physiological role as lipoprotein receptor. *EMBO J 7*:4119–4127.

Herz J, Kowal RC, Goldstein JL, Brown MS. 1990. Proteolytic processing of the 600kD low density lipoprotein receptor-related protein (LRP) occurs ina trans-Golgi compartment. *EMBO J 9*:1769–1776.

Holtet TL, Nielsen KL, Etzerodt M, Moestrup SK, Gliemann J, Sottrup-Jensen L, Thogersen HC. 1994. Recombinant α_2M receptor binding domain binds to the α_2M receptor with high affinity. *Ann NY Acad Sci 737*:480–482.

Horn IR, Van den Berg BMM, Van der Meijden PZ, Pannekoek H, van Zonneveld AJ. 1997. Molecular analysis of ligand binding to the second cluster of complement-type repeats of the low density lipoprotein receptor-related protein: Evidence for an allosteric component in receptor-associated protein-mediated inhibition of ligand binding. *J Biol Chem 272*:13608–13613.

Kay LE, Ikura M, Tschudin R, Bax A. 1990. Three-dimensional triple-resonance NMR spectroscopy of isotopically enriched proteins. *J Magn Reson 89*:496–514.

Kounnas MZ, Church FC, Argraves WS, Strickland DK. 1996. Cellular internalization and degradation of antithrombin III-thrombin, heparin cofactor II-thrombin, and α_1-antitrypsin-trypsin complexes is mediated by the low density lipoprotein receptor-related protein. *J Biol Chem 271*:6523–6529.

Kounnas MZ, Morris RE, Thompson MR, FitzGerald DJ, Strickland DK, Saelinger CB. 1992. The α_2-macroglobulin receptor/low density lipoprotein-related protein binds and internalizes *Pseudomonas* exotoxin A. *J Biol Chem 267*:12420–12423.

Kowal RC, Herz J, Goldstein JL, Esser V, Brown MS. 1989. Low density lipoprotein receptor-related protein mediates uptake of cholesteryl esters derived from apoprotein E-enriched lipoproteins. *Proc Natl Acad Sci USA 86*:5810–5814.

Kristensen T, Moestrup SK, Gliemann J, Bendtsen L, Sand O, Sottrup-Jensen L. 1990. Evidence that the newly cloned low density lipoprotein receptor-related protein (LRP) is the α-2-macroglobulin receptor. *FEBS Lett 276*:151–155.

Manavalan P, Johnson WC Jr. 1987. Variable selection method improves the prediction of protein secondary structure from circular dichroism spectra. *Anal Biochem 167*:76–85.

Maxfield FR. 1982. Weak bases and ionophores rapidly and reversibly raise the pH of endocytic vesicles in cultured mouse fibroblasts. *J Cell Biol 95*:676–681.

Maxfield FR, Willingham MC, Haigler HT, Dragsten P, Pastan I. 1981. Binding, surface mobility, internalization, and degradation of rhodamine-labeled α_2-macroglobulin. *Biochemistry 20*:5353–5358.

Moestrup SK, Kaltoft K, Sottrup-Jensen L, Gliemann J. 1990. The human α_2-macroglobulin receptor contains high affinity calcium binding sites important for receptor conformation and ligand recognition. *J Biol Chem 265*:12623–12628.

Muhandiram DR, Kay LE. 1994. Gradient-enhanced triple resonance 3-dimensional NMR experiments with improved sensitivity. *J Magn Reson Ser B 103*:203–216.

Nielsen KL, Holtet TL, Etzerodt M, Moestrup SK, Gliemann J, Sottrup-Jensen L, Thogersen HC. 1996. Identification of residues in α-macroglobulins important for binding to the α_2-macroglobulin receptor low density lipoprotein receptor-related protein. *J Biol Chem 271*:12909–12912.

Nielsen MS, Nykjaer A, Warshawsky I, Schwartz AL, Gliemann J. 1995. Analysis of ligand binding to the α_2-macroglobulin receptor low density lipoprotein receptor-related protein: Evidence that lipoprotein lipase and the carboxyl-terminal domain of the receptor-associated protein bind to the same site. *J Biol Chem 270*:23713–23719.

Nykjær A, Bengtsson-Olivecrona G, Lookene A, Moestrup SK, Petersen CM, Weber W, Beisiegel U, Gliemann J. 1993. The alpha(2)-macroglobulin receptor/low density lipoprotein receptor-related protein binds lipoprotein lipase and beta-migrating very low density lipoprotein associated with the lipase. *J Biol Chem 268*:15048–15055.

Nykjær A, Petersen CM, Møller B, Jensen PH, Moestrup SK, Holtet TL, Etzerodt M, Thøgersen HC, Munch M, Andreasen PA, Gliemann J. 1992. Purified α_2-macroglobulin receptor/LDL receptor-related protein binds urokinase·plasminogen activator inhibitor type-1 complex. Evidence that the α_2-macroglobulin receptor mediates cellular degradation of urokinase receptor-bound complexes. *J Biol Chem 267*:14543–14546.

Orth K, Madison EL, Gething M-J, Sambrook JF, Herz J. 1992. Complexes of tissue-type plasminogen activator and its serpin inhibitor plasminogen activator inhibitor type 1 are internalized by means of the low density lipoprotein-related protein/α_2-macroglobulin receptor. *Proc Natl Acad Sci USA 89*:7422–7426.

Palmer AG III, Cavanagh J, Wright PE, Rance M. 1991. Sensitivity improvement in proton-detected 2-dimensional heteronuclear correlation NMR spectroscopy. *J Magn Reson 93*:151–170.

Poller W, Willnow TE, Hilpert J, Herz J. 1995. Differential recognition of α_1-antitrypsin-elastase and α_1-antichymotrypsin-cathepsin G complexes by the low density lipoprotein receptor-related protein. *J Biol Chem 270*:2841–2845.

Rost B, Sander C. 1993a. Prediction of protein secondary structure at better than 70% accuracy. *J Mol Biol 232*:584–599.

Rost B, Sander C. 1993b. Improved prediction of protein secondary structure by use of sequence profiles and neural networks. *Proc Natl Acad Sci USA 90*:7558–7562.

Rost B, Sander C. 1994. Combining evolutionary information and neural networks to predict protein secondary structure. *Proteins 19*:55–72.

Rost B, Sander C, Schneider R. 1994. PHD—An automatic mail server for protein secondary structure prediction. *CABIOS 10*:53–60.

Sottrup-Jensen L. 1989. α-Macroglobulins. Structure, shape, and mechanism of proteinase complex formation. *J Biol Chem 264*:11539–11542.

Sottrup-Jensen L, Gliemann J, Van Leuven F. 1986. Domain structure of human α_2-macroglobulin. Characterization of a receptor-binding domain obtained by digestion with papain. *FEBS Lett 205*:20–24.

Strickland DK, Ashcom JD, Williams S, Burgess WH, Migliorini M, Argraves WS. 1990. Sequence identity between the α_2-macroglobulin receptor and low density lipoprotein receptor-related protein suggests that this molecule is a multifunctional receptor. *J Biol Chem 265*:17401–17404.

Strickland DK, Kounnas MZ. 1997. Mechanisms of cellular uptake of thrombin-antithrombin II complexes: Role of the low-density lipoprotein receptor-related protein as a serpin-enzyme complex receptor. *Trends Cardiovasc Med 7*:9–16.

Strickland DK, Kounnas MZ, Argraves WS. 1995. LDL receptor-related protein: A multiligand receptor for lipoprotein and proteinase catabolism. *FASEB J 9*:890–898.

Tapon-Bretaudiere J, Bros A, Couture-Tosi E, Delain E. 1985. Electron microscopy of the conformational changes of α_2-macroglobulin from human plasma. *EMBO J 4*:85–89.

Van Leuven F, Marynen P, Sottrup-Jensen L, Cassiman J-J, Van den Berghe H. 1986. The receptor-binding domain of human α_2-macroglobulin. Isolation after limited proteolysis with a bacterial proteinase. *J Biol Chem 261*:11369–11373.

Williams SE, Ashcom JD, Argraves WS, Strickland DK. 1992. A novel mechanism for controlling the activity of α_2-macroglobulin receptor/low density lipoprotein receptor-related protein: multiple regulatory sites for 39kDa receptor associated protein. *J Biol Chem 267*:9035–9040.

Willnow TE, Goldstein JL, Orth K, Brown MS, Herz J. 1992. LDL receptor related protein and gp330 bind similar ligands, including plasminogen activator-inhibitor complexes and lactoferrin, an inhibitor of chylomicron remnant clearance. *J Biol Chem 267*:26172–26180.

Wilson C, Wardell MR, Weisgraber KH, Mahley RW, Agard DA. 1991. Three-dimensional structure of the LDL receptor-binding domain of human apolipoprotein E. *Science 252*:1817–1822.

Wishart DS, Sykes BD, Richards FM. 1992. The chemical shift index: A fast and simple method for the assignment of protein secondary structure through NMR spectroscopy. *Biochemistry 31*:1647–1651.

Wittekind M, Müller L. 1993. HNCACB, a high sensitivity 3D NMR experiment to correlate amide-proton and nitrogen resonances with the alpha-carbon and beta-carbon resonances in proteins. *J Magn Reson Ser B 101*:201–205.

Wüthrich K. 1986. *NMR of proteins and nucleic acids*. New York: Wiley. 292 pp.

Yamashiro DJ, Borden LA, Maxfield FR. 1989. Kinetics of α_2-macroglobulin endocytosis and degradation in mutant and wild-type Chinese hamster ovary cells. *J Cell Physiol 139*:377–382.